

Royal jelly maintains epidermal stem cell properties by repressing senescence

Mariko Moriyama

Kindai University

Yuko Miyake

Kindai University

Tomomi Degawa

Yamada Bee Company Inc.

Nobuaki Okumura

Yamada Bee Company Inc.

Hiroyuki Moriyama (✉ moriyama@phar.kindai.ac.jp)

Kindai University

Article

Keywords:

Posted Date: September 28th, 2022

DOI: <https://doi.org/10.21203/rs.3.rs-2098858/v1>

License:   This work is licensed under a Creative Commons Attribution 4.0 International License.

[Read Full License](#)

Abstract

Royal jelly (RJ), a natural product secreted by honeybees, is used in various topical products for skincare and aids in maintaining cutaneous homeostasis. However, the mechanism underlying the effect of RJ on the skin has not yet been fully explored. Our previous data indicated that the epidermal equivalents become thicker and contain more p63-expressing proliferative cells after the addition of RJ to the medium. Therefore, we examined the effect of RJ on the proliferative ability of human primary epidermal keratinocytes (HPEKs) in a two-dimensional culture here. We observed only a slight increase in the proliferation of cells with the addition of RJ, suggesting that it is not actively involved in the proliferation of HPEKs. However, population doubling was enhanced in the RJ-treated group in the long-term culture experiment, indicating that RJ inhibits senescence. Additionally, RJ suppressed cellular senescence by regulating the expression levels of Δ Np63, p16, and p21. These results were further confirmed by the presence of major fatty acids, such as 10-hydroxy-2-decenoic acid, in RJ. Overall, our data indicate that RJ can maintain epidermal stem cell properties by repressing senescence.

Introduction

Epidermis is the outermost layer of the skin that plays a crucial role in protecting the body from various environmental stresses. It also has social significance because of its visibility. Hence, the condition of the epidermis has a significant impact on the quality of life in both physiological and psychological aspects.

Epidermis is divided into four layers based on the position and morphology: basal, spinous, granular, and cornified [1]. Epidermal stem/progenitor cells reside in the basal layer of the epidermis, where they proliferate and generate committed cells that undergo terminal differentiation during skin development and homeostasis. Transcription factor p63 is one of the primary regulators of proliferation within the basal layer of the epidermis [2] as well as a regulator of epidermal senescence [3, 4]. The p63 gene, *TP63*, expresses two different types of proteins: the full-length p63 isoform (TAp63) and N-terminal truncated p63 isoform (Δ Np63) proteins [5, 6]. Δ Np63 is the main isoform detected in the basal layers, which regulates the proliferation and inhibits the differentiation of keratinocytes, thereby contributing to the maintenance of keratinocyte stemness [2]. Δ Np63 also blocks keratinocyte senescence by inhibiting the p16^{ink4a}/p19^{arf} pathways in vitro [7], and the conditional knockout of p63 in mice accelerates premature aging in vivo [3].

Royal jelly (RJ) is a yellowish-white, gel-texture substance secreted from the hypopharyngeal and mandibular glands of honeybees (*Apis mellifera*) that is an essential nutrient for queen bees. Owing to its high nutritional value, RJ is widely used in drugs, food, and cosmetics in many countries [8]. The chemical composition of RJ is 60–70% water, 9–18% proteins, 7.5–23% sugars, 3–8% lipids, and 1.5% other compounds, such as minerals and vitamins [9]. Trans-10-hydroxy-2-decenoic acid (10H2DA) and 10-hydroxydecanoic acid (10HDAA) are the two major unique medium-chain fatty acids in RJ that account for 60–80% of RJ lipids. When these fatty acids are incorporated into the body, they are metabolized and converted to 2-decenedioic acid (2DA) and sebacic acid (SA) [9].

RJ exerts various biological effects, including antibacterial [10], anti-inflammatory [11], antioxidant [12], estrogen-like [13], and anti-aging [14] effects, with minimal side effects. Protease-treated RJ (pRJ), an allergen-free form of RJ whose proteins have been converted to amino acids and peptides, has also been developed and reported to have additional benefits compared to non-protease-treated RJ (nRJ) [11, 15]. Owing to its positive properties, RJ is widely used in topical application medicines and cosmetics, such as ointments used in the treatment of various dermatoses, and moisturizing creams and lotions [16]. Although its mechanism of action remains unclear, recent studies have revealed more precise effects of RJ on the epidermis. Duplan et al. revealed that 10H2DA activates keratinocyte differentiation, restores skin barrier function, and reduces inflammation, resulting in moisturization of the epidermis [17]. Our previous report also indicated that RJ induces NAD(P)H quinone oxidoreductase 1 (NQO1) expression, thus protecting the epidermis from oxidative stress [12]. However, the effect of RJ on the maintenance of epidermal homeostasis has not yet been fully elucidated.

In this study, we investigated the effect of RJ on the maintenance of epidermal homeostasis and the underlying mechanism. Our results show that RJ can maintain epidermal stem cell properties by repressing keratinocyte senescence. RJ and RJ-related fatty acids improved the establishment of a human epidermal equivalent model. Furthermore, we found that RJ repressed the replicative senescence of keratinocytes via upregulation of Δ Np63 and downregulation of p16 and p21 expression levels. These findings are important given the extensive use of RJ products in the cosmetic industry.

Materials And Methods

Reagents

Lyophilized nRJ and pRJ were prepared by Yamada Bee Company Inc. (Okayama, Japan). RJ was standardized with specific amounts of fatty acids 10H2DA and 10HDAA: nRJ contained a minimum of 3.8% 10H2DA and 0.6% 10HDAA, while pRJ contained a minimum of 3.5% 10H2DA and 0.6% 10HDAA. The fatty acid 10H2DA was purchased from Hangzhou Eastbiopharm Co., Ltd. (Hangzhou, China), while 10HDAA was purchased from Combi-Blocks, Inc. (San Diego, CA, USA). Moreover, 2DA was purchased from Sundia MediTech Co., Ltd. (Shanghai, China) and SA was purchased from Sigma-Aldrich Co. LLC. (St. Louis, MO, USA).

Cell culture

Human primary epidermal keratinocytes (HPEKs) were purchased from CELLnTEC (Bern, Switzerland) and maintained in CnT-Prime epithelial proliferation medium (CELLnTEC), according to the manufacturer's protocol. Human epidermal equivalents were generated using CnT-Prime 3D Airlift Medium (CELLnTEC), as previously described [18].

Histology and immunofluorescent analysis

Skin equivalents were fixed in 4% paraformaldehyde, embedded in an optimal cutting temperature compound, frozen, and sectioned at 10 μm thickness. Sections were then subjected to either hematoxylin and eosin (H&E) staining or immunohistochemical analysis as previously described [19]. The following were used as primary antibodies: rabbit polyclonal antibody against Ki67 (1/250; NOVUS Biological, Littleton, CO, USA), rabbit polyclonal antibody against p63 (1/200; SantaCruz, Dallas, TX, USA), and chick polyclonal antibody against keratin 14 (1/1000; BioLegend, San Diego, CA, USA). Staining was performed using specific secondary antibodies conjugated to Alexa Fluor 488, Alexa Fluor 546, or Cy3 (1/1000). Following the final washing step, the slides were mounted with coverslips using ProLong Gold Antifade Mountant with 4, 6-diamino-2-phenylindole (Thermo Fisher Scientific, Waltham, MA, USA). Light microscopy images were obtained using a microscope (BZ-9000; Keyence, Osaka, Japan). Fluorescence microscopy images were obtained using a confocal microscope (LSM 800, Carl Zeiss).

Cell viability assay

HPEKs were seeded into a 96-well plate and incubated for 24 h in a 5% CO_2 incubator. The cells were treated with nRJ or pRJ for 48 h. The cell viability assay was performed using Cell Counting Reagent SF (Nacalai Tesque, Kyoto, Japan), according to the manufacturer's protocol. The absorbance of the resultant formazan was measured at 450 nm using a Nivo microplate reader (Perkin Elmer, Waltham, MA, USA).

5-ethynyl-2-deoxyuridine (EdU) proliferation assay

HPEKs were seeded in a 35 mm dish at a density of 5×10^3 cells/ cm^2 and incubated for 24 h in a 5% CO_2 incubator. HPEKs were then treated with nRJ or pRJ for 48 h. After treatment, EdU labeling and detection were performed using the Click-iT EdU Alexa Fluor 488 Flow Cytometry Assay Kit (Thermo Fisher Scientific), according to the manufacturer's instructions. The cells were analyzed using flow cytometry (ec800 cell analyzer; SONY, Tokyo, Japan). FlowJo 10 software (Tree Star Inc., Ashland, OR, USA) was used for quantitative analysis.

RNA extraction, cDNA generation, and quantitative polymerase chain reaction (qPCR)

HPEKs were seeded into a 12-well plate and incubated for 24 h in a 5% CO_2 incubator. HPEKs were then treated with nRJ or pRJ for 72 h. Total RNA was extracted using an RNeasy Mini Kit (Qiagen, Hilden, Germany), according to the manufacturer's instructions. cDNA was generated from 1 μg of total RNA using a Verso cDNA Synthesis Kit (Thermo Scientific) and purified using a MinElute PCR Purification Kit (Qiagen). qPCR analysis was conducted using THUNDERBIRD Next SYBR qPCR Mix (TOYOBO, Osaka, Japan), according to the manufacturer's protocols. The relative expression value of each gene was calculated using the $\Delta\Delta\text{Ct}$ method, and the most reliable internal control gene was determined using the geNorm software (Biogazelle, Zwijnaarde, Belgium). All primers used in this study are listed in Table 1.

Western blotting analysis

HPEKs were seeded into a 6-well plate and incubated for 24 h in a 5% CO₂ incubator. HPEKs were then treated with nRJ or pRJ for 72 h. Cells were lysed with lysis buffer (20 mM Tris-HCl [pH 8.0], 1% SDS, and 1 mM DTT). Blots were probed with mouse monoclonal antibodies against p63 (clone 4A4) (Abcam, Cambridge, UK; ab735) and actin (clone C4) (Merck-Millipore, Billerica, MA, USA; MAB1501). Horseradish peroxidase (HRP)-conjugated anti-mouse IgG secondary antibody (Cell Signaling Technology; #7076) was used as a probe, and immunoreactive bands were visualized using the Immobilon Western Chemiluminescent HRP substrate (Merck-Millipore). Band intensity was measured using the ImageJ 1.49 software (National Institutes of Health, Bethesda, MD, USA).

Statistical analysis

Statistical differences were determined using one-way analysis of variance followed by Dunnett's or Tukey's test using the GraphPad Prism 9 software (GraphPad Software, La Jolla, CA, USA). A value of $P < 0.05$ was considered to be statistically significant ($****P < 0.0001$, $***P < 0.001$, $**P < 0.01$, $*P < 0.05$).

Results

RJ is beneficial for epidermal development

To evaluate the effects of RJ on epidermal development, a human epidermal equivalent model was constructed in a culture medium containing RJ. In this study, lyophilized raw nRJ and pRJ, whose proteins were hydrolyzed using proteases, were used. As shown in Fig. 1A and B, H&E staining revealed that the thickness of the epidermis was significantly enhanced in the human epidermal equivalent model treated with nRJ or pRJ. Ki-67 is a cell proliferation marker and p63 is an important molecule for the maintenance of keratinocyte proliferative activity. We found that the number of p63- and Ki-67-positive cells was significantly increased in nRJ- or pRJ-treated epidermal skin equivalents (Fig. 1C), indicating that the proliferation of undifferentiated basal cells was promoted by the addition of RJ. These data suggest that RJ application facilitates epidermal development by improving the epidermal stem cell properties.

RJ has no immediate effect on keratinocyte proliferation

Next, we evaluated the effects of RJ on cell proliferation in a two-dimensional culture of HPEKs. Water-soluble tetrazolium salt (WST)-8 assay revealed that the number of living cells was slightly increased (approximately 1.1-fold and 1.4-fold in 10 µg/mL nRJ- and 100 µg/mL pRJ-treated cells and 10 µg/mL pRJ-treated cells, respectively) when treated with nRJ or pRJ (Fig. 2A); however, no significant difference was observed. To directly evaluate the rate of DNA synthesis in HPEKs, nuclear incorporation of EdU was also examined. As shown in Fig. 2B, an approximate 1.1-fold increase in EdU intake was observed in RJ-treated cells. These data suggest that RJ is not actively involved in the promotion of cell proliferation.

RJ suppresses the replicative senescence of keratinocytes

Cellular senescence is one possible reason for reduced stem cell function. Therefore, we attempted to measure the population doubling level of HPEKs by culturing them for a long time. Control HPEKs reached their limit of cell proliferation at the earliest. In contrast, both nRJ and pRJ treatments increased the proliferative capacity of HPEKs (Fig. 3A). In addition, control HPEKs at day 42 showed characteristics typical of senescence, that is, large and flat cell morphology, whereas RJ-treated HPEKs still showed small and cobblestone-like morphology (Fig. 3B). These data indicate that RJ suppresses senescence, thereby aiding in the maintenance of the stem cell properties of HPEKs.

RJ upregulates Δ Np63 and suppresses p16 and p21 expression levels in keratinocytes

Next, we evaluated the expression levels of Δ Np63 and several cellular senescence markers to understand the mechanism by which RJ suppresses senescence in HPEKs. To detect *TP63* mRNA expression, we used primer pairs specific for the sequence encoding Δ Np63 isoforms. qPCR analysis revealed that RJ significantly increased the expression of Δ Np63 (Fig. 4A). Western blotting analysis also revealed a significant increase in Δ Np63 α protein expression in RJ-treated HPEKs (Fig. 4B). Furthermore, we found that the mRNA expression levels of cyclin-dependent kinase inhibitor 1A (*CDKN1A*; p21) and *CDKN2A* (p16) in HPEKs were significantly repressed by both nRJ and pRJ treatment (Fig. 4C). These data suggest that RJ suppresses cellular senescence by regulating Δ Np63, p16, and p21 expression levels.

RJ-related fatty acids are beneficial for epidermal development

Next, we identified the specific factors in RJ that are responsible for its beneficial effects on HPEKs. Our results revealed that pRJ, a protease-hydrolyzed RJ, is involved in suppressing keratinocyte senescence and regulating the gene expression of *Δ Np63*, *p16*, and *p21* at levels similar to that maintained by nRJ (Figs 1–4), indicating that the protein components in RJ do not contribute to these effects. Therefore, we investigated the effects of 10H2DA and 10HDAA, which are medium-chain fatty acids characteristic of RJ, and their metabolites, 2DA and SA [9], on the development of epidermal equivalents. As shown in Fig. 5A and B, the addition of 10H2DA, 10HDAA, 2DA, and SA resulted in significant epidermal thickening in the human epidermal equivalent model. Moreover, 10H2DA was found to be the most effective fatty acid (Fig. 5B). We also found that the number of p63- and Ki-67-positive cells was significantly increased in fatty acid-treated epidermal equivalents (Fig. 5C), similar to that in the RJ-treated equivalents (Fig. 1C).

Discussion

RJ is widely used in traditional medicine and cosmetics; however, its effects on epidermal keratinocytes have not yet been elucidated. In the present study, we used molecular and cellular approaches to generate scientific data on the effects of RJ on epidermal keratinocytes. Our results indicate that RJ may exert beneficial effects on the maintenance of epidermal stem cell properties by suppressing senescence. We found that RJ and RJ-related fatty acids significantly thickened the human epidermal equivalent (Figs. 1 and 5). Moreover, the beneficial effect was not due to enhanced HPEK proliferation by RJ (Fig. 2), but due to the suppression of replicative senescence of HPEKs (Fig. 3).

RJ exerts anti-aging effects in various species [20, 21]. Senescence is caused by various stresses, such as the accumulation of reactive oxygen species, damage to telomeres, activation of oncogenes, and dysfunction of mitochondria. The main characteristic of senescence can be defined as a stable growth arrest, which is implemented by the activation of p16^{INK4a} and p53/p21^{CIP1} tumor suppressor networks [22]. In this study, we found that RJ suppressed cellular senescence by inhibiting *CDKN1A* (p21) and *CDKN2A* (p16) expression levels in HPEKs (Figs. 3 and 4). Although the mechanism by which RJ contributes to the inhibition of these genes could not be determined in the present study, it is possible that the antioxidant activity of RJ contributes to the repression of p21 and p16 expression. We previously reported that RJ induced the expression of NQO1 and protected the skin against oxidative stress [12]. However, as these effects were attributed solely to 10H2DA rather than 10HDAA, the antioxidant effect of elevated NQO1 expression does not seem to be the main reason for the inhibition of p16 and p21 expression levels by RJ treatment, although it may have a little effect on the present results. Another possible mechanism by which RJ suppresses p16 and p21 expression is the upregulation of Δ Np63 expression (Figs. 1 and 4). p63 is a transcription factor that belongs to the *p53* gene family. The N-terminal truncated p63 isoform, Δ Np63 α , is the main isoform detected in the basal layer and has the ability to directly bind to the p16, p19, and p21 promoters to repress their expression and prevent cellular senescence [7, 23, 24]. Moses et al. also indicated that histone deacetylase-1/2 together with Δ Np63 is required for the suppression of p21 and p16 in undifferentiated keratinocytes [25]. However, further experiments are required to determine whether the increase in Δ Np63 expression induced by RJ contributes to the direct suppression of *CDKN1A* (p21) and *CDKN2A* (p16) expression levels.

RJ contains approximately 4% 10H2DA and 1.5% 10HDAA, which are unique medium-chain fatty acids. In this study, the maximum concentration of RJ used in the 3D culture was 400 μ g/mL. The concentration of 10H2DA, the most abundant fatty acid in RJ, at 400 μ g/mL RJ was calculated to be approximately 86 μ M. Therefore, we treated keratinocytes with 80 μ M of each fatty acid (10H2DA, 10HDAA, 2DA, and SA) in the 3D culture. Our data revealed that all fatty acids investigated in this study (10H2DA, 10HDAA, 2DA, and SA) contributed to the enhancement of epidermal thickness equivalent to levels comparable to RJ, indicating that these fatty acids are active compounds in this reaction (Fig. 5). The concentrations of 2DA and SA in RJ are much lower than those of 10H2DA and 10HDAA, and 2DA and DA are metabolized from 10H2DA and 10HDAA, respectively, *in vivo* [9]. Therefore, RJ administration is expected to be effective in maintaining epidermal homeostasis even after metabolism *in vivo*.

Traditionally, RJ is used for the improvement of menopause-related symptoms [8]. Therefore, the estrogenic activity of RJ has attracted attention and its efficacy has been investigated. RJ enhances the proliferation of estrogen-sensitive breast cancer cell line, MCF-7 and upregulates the transcription of genes dependent on the estrogen-responsive element via interaction with estrogen receptors (ERs) [13]. Suzuki et al. reported that 10H2DA, 10HDAA, and 2DA bind to the ER- β , thereby enhancing the ER response [26]. In addition, Moutsatsou et al. also reported that fatty acids of RJ, such as 10H2DA, SA, and 3,10-dihydroxydecanoic, present strong estrogenic effects that mediate estrogen signaling by modulating the recruitment of ERs and co-activators to the target genes [27]. Estrogen also affects various skin

conditions. Application of 17 β -estradiol, the most potent estrogen, increases the proliferative capacity of epidermal keratinocytes in both humans and mice, resulting in a thicker epidermis [28–30]. Therefore, the estrogenic activities of fatty acids in RJ may contribute to the beneficial effects on epidermal keratinocytes as indicated in the present study. However, the estrogenic activity of RJ remains ambiguous as a recent study indicated that RJ exhibited little or no estrogenic activity via ER-mediated genomic signaling pathway both *in vitro* and *in vivo* [31]. This point needs to be investigated further in future studies.

Overall, this study provides the first evidence that RJ has a positive impact on epidermal keratinocytes by maintaining their stem cell properties via senescence inhibition. The main advantage of bee-based cosmetics is their high efficacy, with minimal side effects. Hence, RJ can potentially be used as a functional cosmetic ingredient.

Declarations

Acknowledgments

We thank Ayumu Morioka and Taiki Higuchi for their technical assistance in this study. We also thank Editage for English language editing.

Author Contributions

M.M., N.O., and H.M. designed the experiments and interpreted the data. M.M., Y.M., and T.D. performed most of the experiments and analyses. T.D. and N.O. provided the RJ samples. M.M. and H.M. were responsible for writing the manuscript. All authors read and agreed to the final version of the manuscript.

Data availability statement

All data generated or analyzed during this study are included in this published article.

Competing Interests

Mariko Moriyama, Yuko Miyake, and Hiroyuki Moriyama declare no competing interests. Tomomi Degawa and Nobuaki Okumura are employees of Yamada Bee Company Inc.

References

1. FM Watt. Terminal differentiation of epidermal keratinocytes. *Curr Opin Cell Biol.* 1989;1(6):1107–15.
2. M Senoo, F Pinto, CP Crum and F McKeon. p63 Is essential for the proliferative potential of stem cells in stratified epithelia. *Cell.* 2007;129(3):523–36.
3. WM Keyes, Y Wu, H Vogel, X Guo, SW Lowe and AA Mills. p63 deficiency activates a program of cellular senescence and leads to accelerated aging. *Genes Dev.* 2005;19(17):1986–99.

4. P Rivetti di Val Cervo, AM Lena, M Nicoloso, S Rossi, M Mancini, H Zhou, et al. p63-microRNA feedback in keratinocyte senescence. *Proceedings of the National Academy of Sciences of the United States of America*. 2012;109(4):1133–8.
5. AB Truong, M Kretz, TW Ridky, R Kimmel and PA Khavari. p63 regulates proliferation and differentiation of developmentally mature keratinocytes. *Genes Dev*. 2006;20(22):3185–97.
6. E Candi, A Rufini, A Terrinoni, D Dinsdale, M Ranalli, A Paradisi, et al. Differential roles of p63 isoforms in epidermal development: selective genetic complementation in p63 null mice. *Cell Death Differ*. 2006;13(6):1037–47.
7. L Ha, RM Ponnampuruma, S Jay, MS Ricci and WC Weinberg. Dysregulated DeltaNp63alpha inhibits expression of Ink4a/arf, blocks senescence, and promotes malignant conversion of keratinocytes. *PloS one*. 2011;6(7):e21877.
8. A Balan, MA Moga, L Dima, S Toma, A Elena Neculau and CV Anastasiu. Royal Jelly-A Traditional and Natural Remedy for Postmenopausal Symptoms and Aging-Related Pathologies. *Molecules*. 2020;25(14).
9. M Yamaga, H Tani, A Yamaki, T Tatefuji and K Hashimoto. Metabolism and pharmacokinetics of medium chain fatty acids after oral administration of royal jelly to healthy subjects. *RSC Adv*. 2019;9(27):15392–401.
10. M Sediva, M Laho, L Kohutova, A Mojzisova, J Majtan and J Klaudivny. 10-HDA, A Major Fatty Acid of Royal Jelly, Exhibits pH Dependent Growth-Inhibitory Activity Against Different Strains of *Paenibacillus* larvae. *Molecules*. 2018;23(12).
11. H Gu, I-B Song, H-J Han, N-Y Lee, J-Y Cha, Y-K Son, et al. Anti-inflammatory and immune-enhancing effects of enzyme-treated royal jelly. *Applied Biological Chemistry*. 2018;61(2):227–33.
12. N Okumura, T Ito, T Degawa, M Moriyama and H Moriyama. Royal Jelly Protects against Epidermal Stress through Upregulation of the NQO1 Expression. *Int J Mol Sci*. 2021;22(23).
13. S Mishima, KM Suzuki, Y Isohama, N Kuratsu, Y Araki, M Inoue, et al. Royal jelly has estrogenic effects in vitro and in vivo. *J Ethnopharmacol*. 2005;101(1–3):215–20.
14. H Kunugi and A Mohammed Ali. Royal Jelly and Its Components Promote Healthy Aging and Longevity: From Animal Models to Humans. *Int J Mol Sci*. 2019;20(19).
15. T Nagai, R Inoue, N Suzuki and T Nagashima. Antioxidant properties of enzymatic hydrolysates from royal jelly. *J Med Food*. 2006;9(3):363–7.
16. A Kurek-Gorecka, M Gorecki, A Rzepecka-Stojko, R Balwierz and J Stojko. Bee Products in Dermatology and Skin Care. *Molecules*. 2020;25(3).
17. H Duplan, E Questel, H Hernandez-Pigeon, MF Galliano, A Caruana, I Ceruti, et al. Effects of Hydroxydecine((R)) (10-hydroxy-2-decenoic acid) on skin barrier structure and function in vitro and clinical efficacy in the treatment of UV-induced xerosis. *Eur J Dermatol*. 2011;21(6):906–15.
18. M Moriyama, H Moriyama, J Uda, A Matsuyama, M Osawa and T Hayakawa. BNIP3 plays crucial roles in the differentiation and maintenance of epidermal keratinocytes. *The Journal of investigative dermatology*. 2014;134(6):1627–35.

19. M Moriyama, H Moriyama, J Uda, H Kubo, Y Nakajima, A Goto, et al. Beneficial Effects of the Genus Aloe on Wound Healing, Cell Proliferation, and Differentiation of Epidermal Keratinocytes. *PloS one*. 2016;11(10):e0164799.
20. Y Honda, Y Fujita, H Maruyama, Y Araki, K Ichihara, A Sato, et al. Lifespan-extending effects of royal jelly and its related substances on the nematode *Caenorhabditis elegans*. *PloS one*. 2011;6(8):e23527.
21. N Okumura, T Toda, Y Ozawa, K Watanabe, T Ikuta, T Tatefuji, et al. Royal Jelly Delays Motor Functional Impairment During Aging in Genetically Heterogeneous Male Mice. *Nutrients*. 2018;10(9).
22. D McHugh and J Gil. Senescence and aging: Causes, consequences, and therapeutic avenues. *The Journal of cell biology*. 2018;217(1):65–77.
23. X Su, MS Cho, YJ Gi, BA Ayanga, CJ Sherr and ER Flores. Rescue of key features of the p63-null epithelial phenotype by inactivation of Ink4a and Arf. *EMBO J*. 2009;28(13):1904–15.
24. MD Westfall, DJ Mays, JC Sniezek and JA Pietenpol. The Delta Np63 alpha phosphoprotein binds the p21 and 14-3-3 sigma promoters in vivo and has transcriptional repressor activity that is reduced by Hay-Wells syndrome-derived mutations. *Molecular and cellular biology*. 2003;23(7):2264–76.
25. M LeBoeuf, A Terrell, S Trivedi, S Sinha, JA Epstein, EN Olson, et al. Hdac1 and Hdac2 act redundantly to control p63 and p53 functions in epidermal progenitor cells. *Developmental cell*. 2010;19(6):807–18.
26. KM Suzuki, Y Isohama, H Maruyama, Y Yamada, Y Narita, S Ohta, et al. Estrogenic activities of Fatty acids and a sterol isolated from royal jelly. *Evid Based Complement Alternat Med*. 2008;5(3):295–302.
27. P Moutsatsou, Z Papoutsis, E Kassi, N Heldring, C Zhao, A Tsiapara, et al. Fatty acids derived from royal jelly are modulators of estrogen receptor functions. *PloS one*. 2010;5(12):e15594.
28. S Verdier-Sevrain, M Yaar, J Cantatore, A Traish and BA Gilchrist. Estradiol induces proliferation of keratinocytes via a receptor mediated mechanism. *FASEB J*. 2004;18(11):1252–4.
29. S Moverare, MK Lindberg, J Faergemann, JA Gustafsson and C Ohlsson. Estrogen receptor alpha, but not estrogen receptor beta, is involved in the regulation of the hair follicle cycling as well as the thickness of epidermis in male mice. *The Journal of investigative dermatology*. 2002;119(5):1053–8.
30. ED Son, JY Lee, S Lee, MS Kim, BG Lee, IS Chang, et al. Topical application of 17beta-estradiol increases extracellular matrix protein synthesis by stimulating tgf-Beta signaling in aged human skin in vivo. *The Journal of investigative dermatology*. 2005;124(6):1149–61.
31. K Ishida, D Matsumaru, S Shimizu, Y Hiromori, H Nagase and T Nakanishi. Evaluation of the estrogenic action potential of royal jelly by genomic signaling pathway in vitro and in vivo. *Biol Pharm Bull*. 2022.

Tables

Table 1. qPCR primers used in this study

Gene		Primer sequence (5'→3')
<i>ΔNp63</i>	F	ATGTTGTACCTGGAAAACAATGC
	R	CTGGAAGGACACGTCGAAACTGTG
<i>CDKN1A</i>	F	GTCACTGTCTTGTACCCTTGTG
	R	CGGCGTTTGGAGTGGTAGAAA
<i>CDKN2A</i>	F	AGCCTTCGGCTGACTGGCTGG
	R	CTGCCCATCATCATGACCTGGA
<i>ACTB</i>	F	CATGTACGTTGCTATCCAGGC
	R	CTCCTTAATGTCACGCACGAT
<i>B2M</i>	F	TATCCAGCGTACTCCAAAGA
	R	GACAAGTCTGAATGCTCCAC
<i>GAPDH</i>	F	CATGAGAAGTATGACAACAGCCT
	R	AGTCCTTCCACGATACCAAAGT
<i>GUS</i>	F	CACCAGGGACCATCCAATACC
	R	GGTACTGCCCTTGACAGAGA
<i>HPRT</i>	F	ATTGTAATGACCAGTCAACAGGG
	R	GCATTGTTTTGCCAGTGTCAA
<i>RN18S</i>	F	ATCATTGGAGGGCAAGTC
	R	GCTCCAAGATCCAACACTACG
<i>UBE2D2</i>	F	TGGCAAGCTACAATAATGGGG
	R	GGAGACCACTGTGATCGTAGA
<i>UBE4A</i>	F	GTACTIONGGGATTTACAGGTTGC
	R	GGCTAGAACTTTGCTGAGCATC

Figures

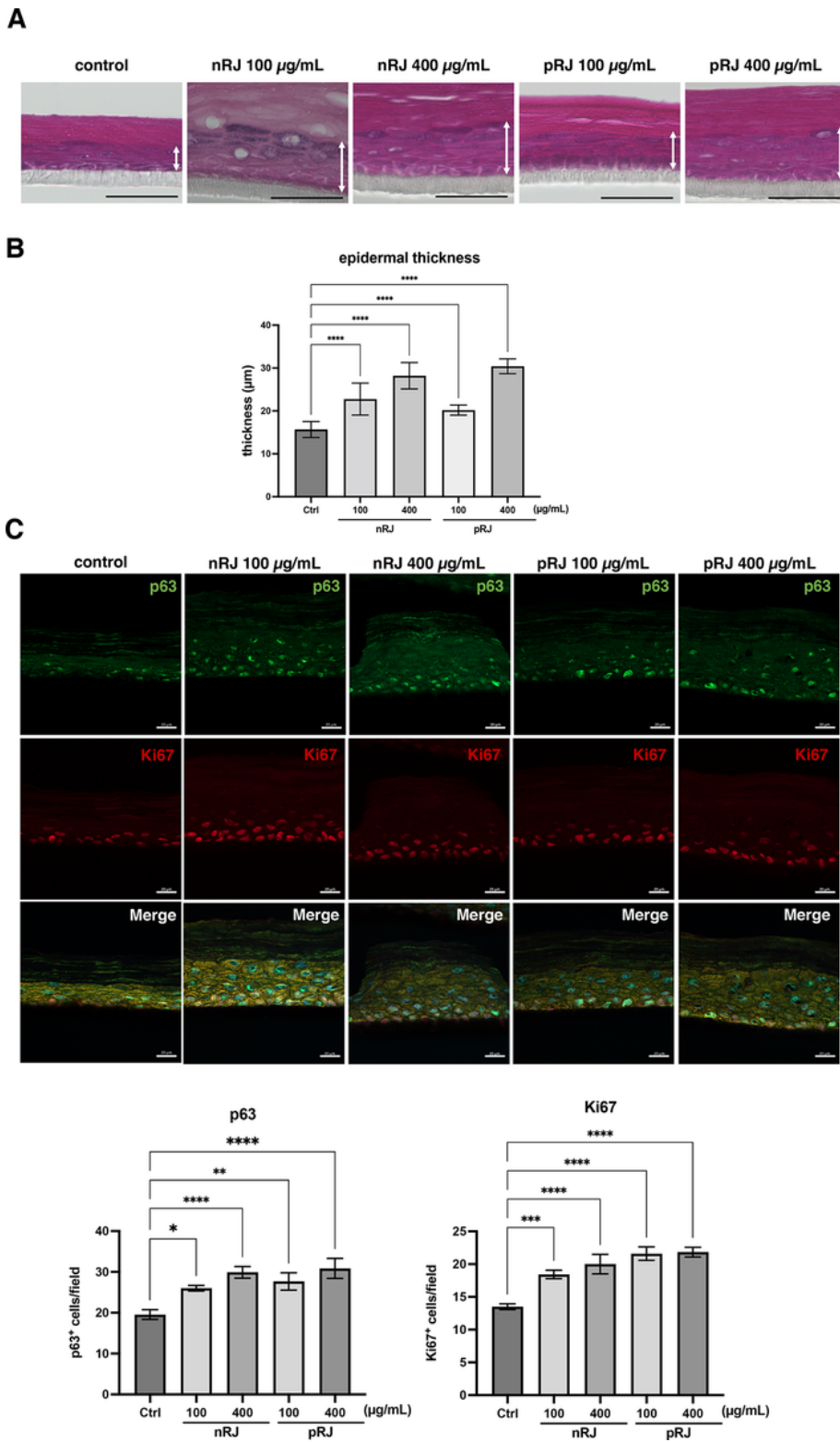


Figure 1

Effect of royal jelly (RJ) on the construction of the human epidermal equivalent model. (**A–C**) Human epidermal equivalent model was developed for 14 d supplemented with non-protease-treated RJ (nRJ) or protease-treated RJ (pRJ). (**A**) Hematoxylin and eosin staining was performed. White double arrow lines indicate the distance from the basal layer to granular layer. Scale bar, 50 µm. (**B**) Graph represents the mean \pm standard deviation (SD) values for the thickness of the epidermis (from basal layer to granular

layer) of the skin equivalent in micrometers from three independent experiments. The thickness was measured in at least 20 representative fields of view per independent experiment. ****P < 0.0001. (C) Immunohistochemical staining against Ki67 (green), p63 (red), and keratin 14 (orange) was performed. Blue signals indicate nuclear staining (4, 6-diamino-2-phenylindole, DAPI). Scale bar, 20 μ m. Graphs represent the mean \pm standard error of the mean (SEM) values for the number of p63- or Ki67-positive cells per field of the skin equivalent from three independent experiments. The positive cells were counted in at least five representative fields of view per independent experiment. ****P < 0.0001, ***P < 0.001, **P < 0.01, *P < 0.05.

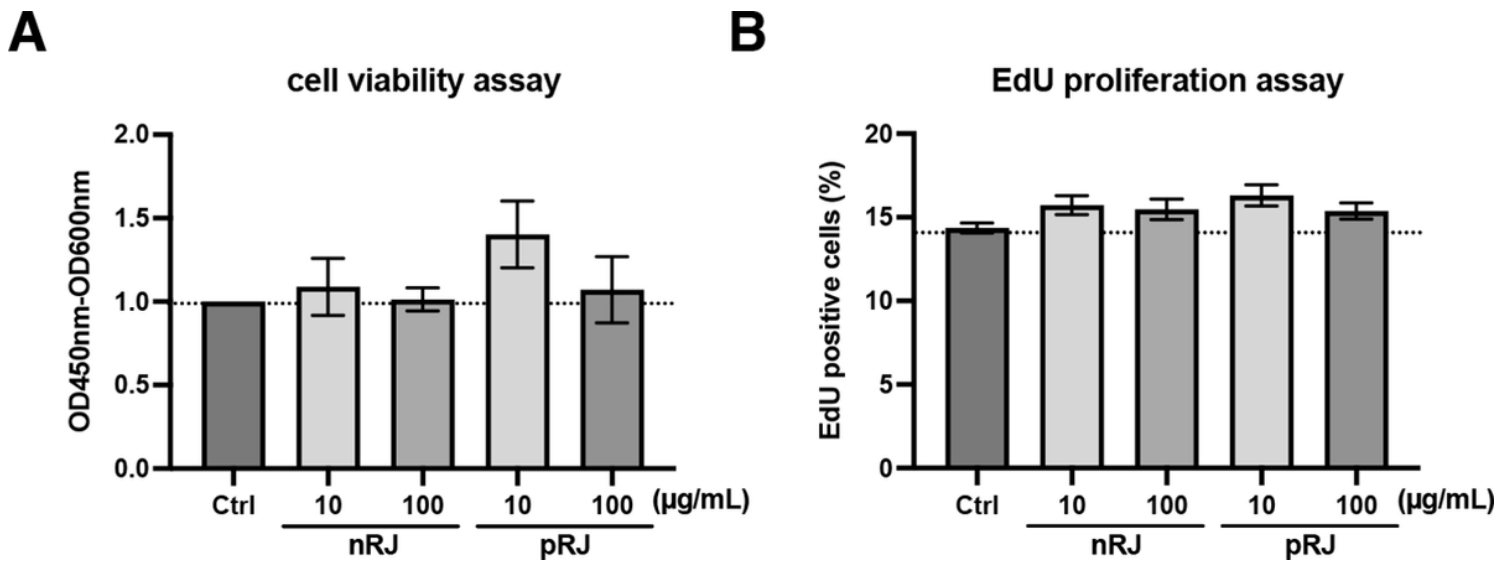


Figure 2

Effect of RJ on the proliferation of human primary epidermal keratinocytes (HPEKs). (A) HPEKs were treated with nRJ or pRJ (10 μ g/mL or 100 μ g/mL) for 48 h and subjected to the cell viability assay. Graphs indicate the mean \pm SEM values (fold increase over control) from eight independent experiments. (B) HPEKs were treated with nRJ or pRJ (10 or 100 μ g/mL) for 48 h and subjected to the 5-ethynyl-2-deoxyuridine (EdU) incorporation assay. Graphs indicate the mean \pm SEM values for percentage of EdU-positive cells from five independent experiments.

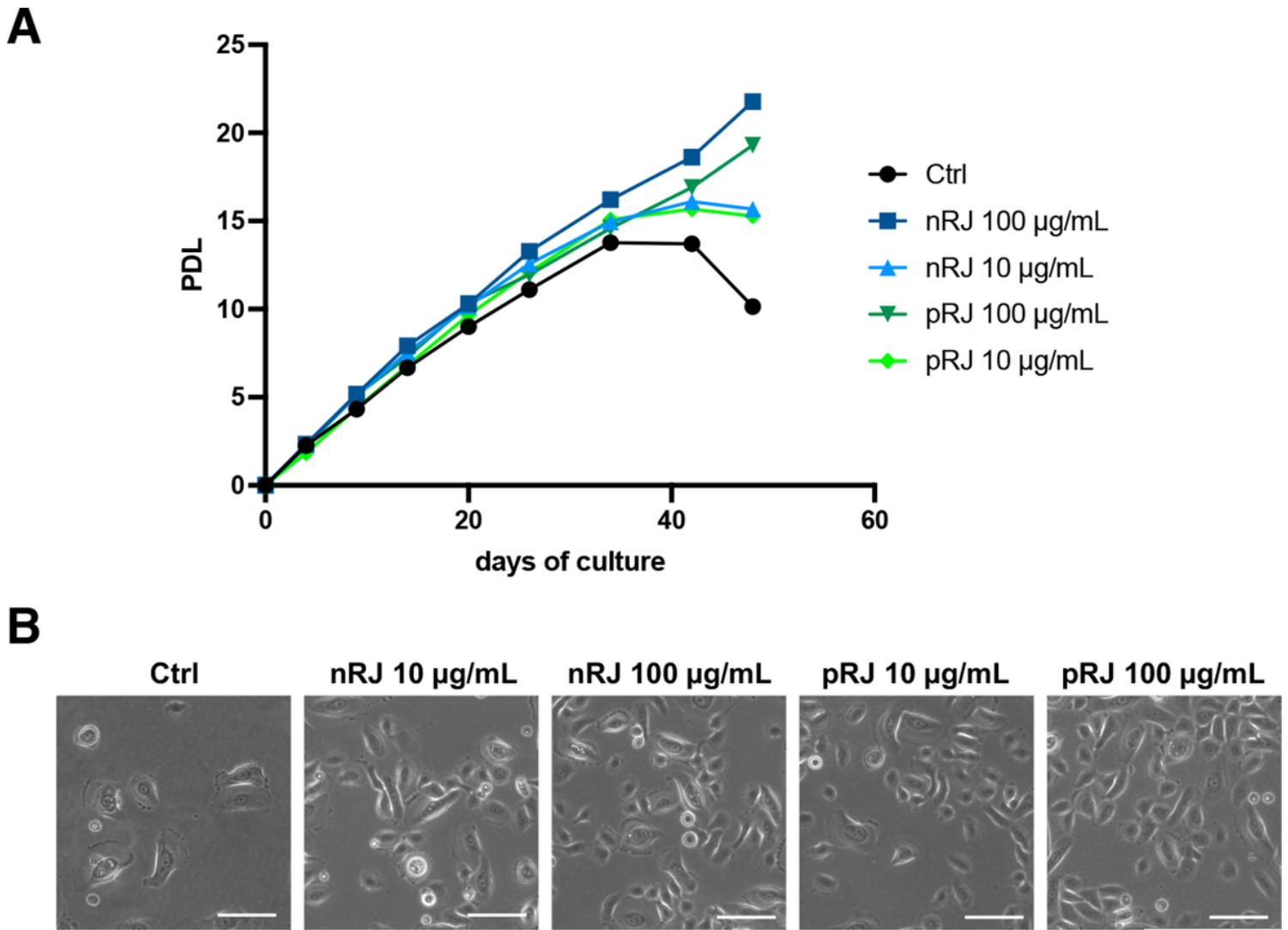


Figure 3

Effect of RJ on the replicative senescence of HPEKs. **(A)** Cumulative population doubling level (PDL) of HPEKs was measured. One representative experiment out of the three experiments performed is shown. **(B)** Representative phase-contrast cell images at day 48. Scale bar, 100 µm.

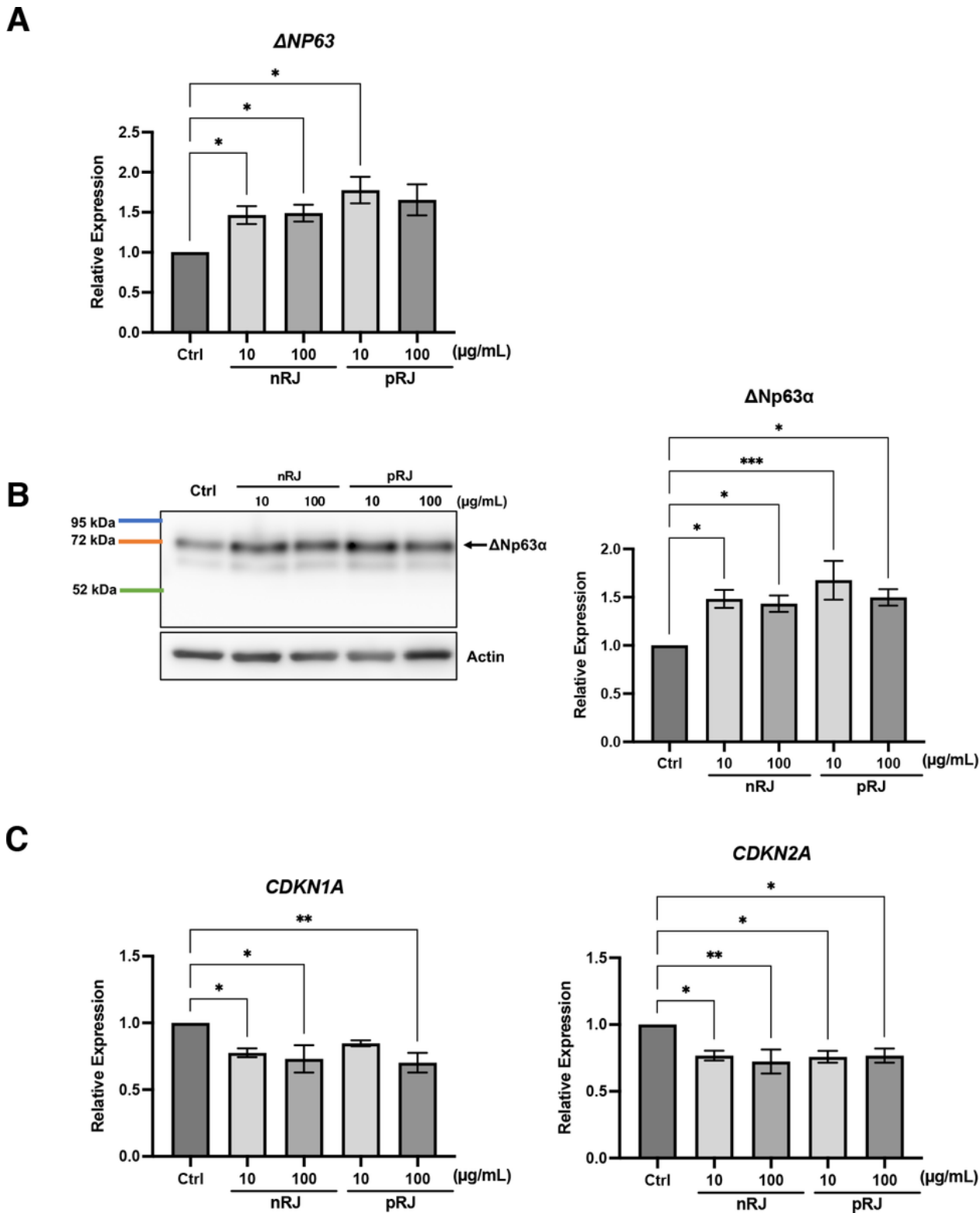


Figure 4

Effect of RJ on the expression levels of epidermal stem cell and senescence markers. (A–C) HPEKs were treated with nRJ or pRJ (10 $\mu\text{g}/\text{mL}$ or 100 $\mu\text{g}/\text{mL}$) for 72 h and subjected to quantitative polymerase chain reaction (qPCR) analysis (A, C) or western blotting analysis (B). (A) Gene expression levels of *ΔNp63* were quantified via qPCR analysis. Graph indicates the mean \pm SEM values for the relative expression from six independent experiments. * $P < 0.05$. (B) Extracted proteins were immunoblotted with

the p63 antibody. Graphs indicate the relative band intensities as determined using the ImageJ software and plotted as the mean of five independent experiments. *** $P < 0.001$, * $P < 0.05$. (C) Gene expression levels of cyclin-dependent kinase inhibitor 1A (*CDKN1A*) and *CDKN2A* were quantified via qPCR analysis. Graphs indicate the mean \pm SEM values for the relative expression from six independent experiments. ** $P < 0.01$, * $P < 0.05$.

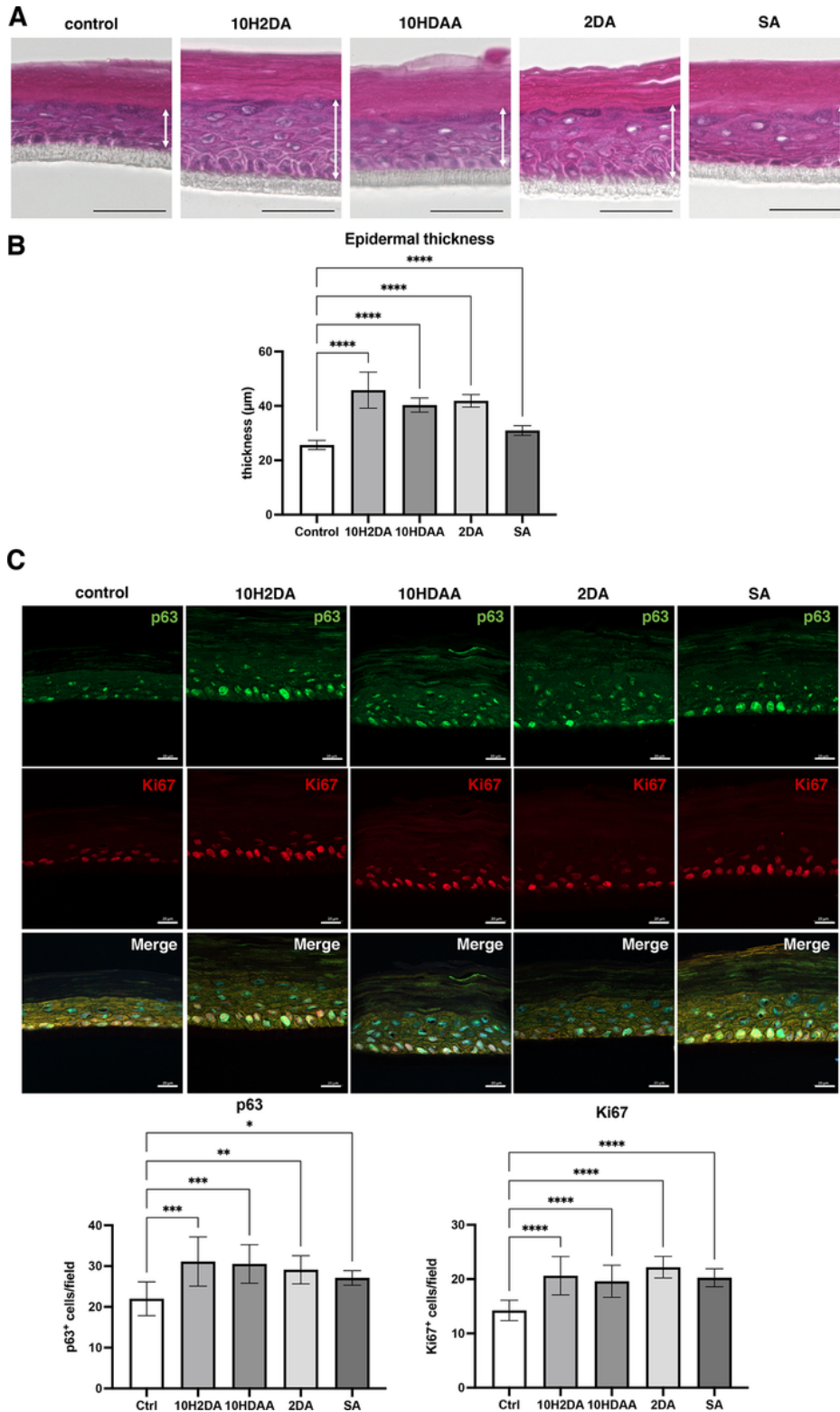


Figure 5

Effects of the fatty acids in RJ on the development of the human epidermal equivalent model. **(A–C)** Human epidermal equivalent model was developed for 14 d supplemented with trans-10-hydroxy-2-decenoic acid (10H2DA), 10-hydroxydecanoic acid (10HDAA), 2-decenedioic acid (2DA), or sebacic acid (SA). **(A)** Hematoxylin and eosin staining was performed. White double arrow lines indicate the distance from the basal layer to granular layer. Scale bar, 50 μm . **(B)** Graphs represent the mean \pm SD values for thickness of the epidermis (from basal layer to granular layer) of the skin equivalent in micrometers from three independent experiments. Thickness was measured in at least 20 representative fields of view per independent experiment. ****P < 0.0001, **P < 0.01. **(C)** Immunohistochemical staining against Ki67 (green), p63 (red), and keratin 14 (orange) was performed. Blue signals indicate nuclear staining (DAPI). Scale bar, 20 μm . Graphs represent the mean \pm SEM values for the number of p63- or Ki67-positive cells per field of the skin equivalent from three independent experiments. Positive cells were counted in at least five representative fields of view per independent experiment. ****P < 0.0001, ***P < 0.001, **P < 0.01, *P < 0.05.